


## CASE STUDY

# Deep cerebral vein expansion with metabolic and neurocognitive recovery in Sturge–Weber syndrome

Flóra John<sup>1</sup>, Mohsin Maqbool<sup>2</sup>, Jeong-won Jeong<sup>1</sup>, Rajkumar Agarwal<sup>1</sup>, Michael E. Behen<sup>1</sup> & Csaba Juhász<sup>1</sup> 

<sup>1</sup>Departments of Pediatrics and Neurology, Wayne State University School of Medicine, Children's Hospital of Michigan, Detroit Medical Center, Detroit, Michigan

<sup>2</sup>Texas Child Neurology, Plano, Texas

## Correspondence

Csaba Juhász, Professor of Pediatrics and Neurology, Wayne State University School of Medicine, PET Center and Translational Imaging Laboratory, Children's Hospital of Michigan, 3901 Beaubien St., Detroit, MI 48201. Tel: 313 966 5136; Fax: 313 966 9228; E-mail: csaba.juhasz@wayne.edu

## Funding Information

This work was supported by grants from the National Institutes of Health (R01 NS041922 to C.J. and R01 NS089659 to J.J.).

Received: 16 January 2018; Revised: 23 January 2018; Accepted: 5 February 2018

*Annals of Clinical and Translational Neurology* 2018; 5(4): 502–506

doi: 10.1002/acn3.546

## Abstract

We present longitudinal imaging data of a child with Sturge–Weber syndrome (SWS). At age 8 months, 3 weeks after initial seizures and prolonged motor deficit, MRI showed extensive right hemispheric SWS involvement with severe glucose hypometabolism on PET. She was treated with levetiracetam and aspirin. Follow-up imaging at age 29 months showed a robust interval expansion of enlarged deep medullary veins throughout the affected hemisphere along with a dramatic recovery of hemispheric metabolism and normalized neurocognitive functioning. These findings demonstrate a robust, multilobar hemispheric remodeling of deep venous collaterals that likely contributed to reversal of initial metabolic and neurocognitive deficits.

## Introduction

Sturge–Weber syndrome (SWS) is a congenital neurocutaneous disorder characterized by facial venous capillary malformation (port-wine birthmark), leptomeningeal venous malformation (angiomas), and glaucoma.<sup>1</sup> Recently, a somatic mutation of the GNAQ gene has been described as the likely cause of the disease.<sup>2</sup> The diagnosis is usually suspected at birth based on the facial port-wine birthmark and then established by neuroimaging; typical SWS brain involvement on MRI includes leptomeningeal contrast enhancement, enlarged deep veins and choroid plexus, focal atrophy, and calcifications.<sup>3</sup> The clinical course and outcome of SWS is highly variable, ranging from no or minimal neurological signs to severe impairment with uncontrolled seizures, hemiparesis, visual field cut, and learning disability.<sup>3</sup> Cross-sectional and longitudinal neuroimaging studies showed that some children

with SWS show good neurocognitive outcome despite extensive unilateral brain involvement, presumably due to early, effective functional reorganization in the contralateral (unaffected) hemisphere.<sup>4–6</sup> In a recent study, using susceptibility-weighted imaging (SWI), an MRI sequence uniquely sensitive to small veins in the brain,<sup>7</sup> we have also demonstrated a modest postnatal expansion of deep medullary veins in the early clinical course of two children with SWS, and its possible protective effect against progressive cortical damage.<sup>8</sup>

Here, we describe a child with SWS who underwent longitudinal multimodal imaging (starting shortly after initial seizures) that demonstrated a robust interval expansion of deep cerebral venous system in the affected right hemisphere during the early disease course coinciding with a dramatic improvement of the initial severe hemispheric hypometabolism and complete normalization of neurocognitive functions.

## Case Report

The girl was born full-term with no complication during pregnancy or at birth. She was diagnosed with SWS due to her extensive port-wine birthmarks covering the right side of her face extending to the scalp and right ear, as well as the right side of her chest and back and the right arm (Fig. 1). Clinical MRI at age 4 months (at another institute) showed extensive leptomeningeal contrast enhancement in the right hemisphere, along with a few enlarged deep medullary veins in the right centrum semiovale on postcontrast T1-weighted images. She was also diagnosed with glaucoma on the right eye. She developed well until 7.5 months of age, when she suffered from repeated episodes of left-sided arm twitching followed by prolonged left arm weakness; and eventually a focal seizure involving left face and left arm twitching and left-sided eye deviation. At that time, levetiracetam (20 mg/kg/day) and aspirin (40.5 mg/day) treatment was started. Three weeks after these seizures (at age 8 months), she underwent multimodal imaging at our hospital as a part of a longitudinal research study approved by the Wayne State University Human Investigation Committee, and written informed consent was obtained from the parents. At that time, she strongly preferred using her right hand, her left arm had a slight spasticity, but her legs appeared symmetric in strength and movements. A 3T MRI (on a Siemens MAGNETOM Verio scanner, with a 32-channel head coil) showed extensive right hemispheric SWS brain involvement with leptomeningeal enhancement on postcontrast T1-weighted images involving portions of all four lobes along with lack or paucity of normal cortical veins extensively (Fig. 2A). SWI (double gradient echo sequence<sup>9</sup>, voxel size:  $0.5 \times$

$0.5 \times 2.0 \text{ mm}^3$ , slice number: 64, acquisition time: 5.0 min) demonstrated several enlarged deep medullary and subependymal veins in the right frontal, parietal, and temporo-occipital regions (Fig. 2C). The right choroid plexus was enlarged, and multilobar atrophy was most prominent in the anterior temporal lobe in the right hemisphere. A PET scan with 2-deoxy-2- $^{18}\text{F}$ fluoro-D-glucose (FDG) showed extensive, severe right hemispheric hypometabolism affecting all four lobes with a relatively preserved medial frontal, and slightly decreased medial parietal and inferior temporal glucose uptake (Fig. 2B). EEG recorded during the FDG uptake period showed right hemispheric attenuation with no epileptiform activity. Caregiver report of adaptive behavioral functioning revealed good communication skills (standard score on Vineland Adaptive Behavior Scale-II [VABS-II] testing: 112), and borderline daily living, socialization, and motor skill scores (72, 77, and 76, respectively).

The child underwent a second, follow-up multimodal imaging and neurocognitive evaluation at 29 months of age. She had no additional clinical seizures since the initial cluster, and her left arm weakness has resolved. Also, she had no spasticity or abnormal reflexes. She had no signs of visual field impairment on clinical examination. Her glaucoma was controlled with eye drops, and she received laser therapy for her facial port-wine birthmark. She has been maintained on levetiracetam 25-30 mg/kg/day divided twice a day and aspirin 40.5 mg daily. SWI performed on the same MRI scanner showed a dramatic interval expansion of the enlarged deep medullary veins encompassing much of the right hemisphere, with multiple enlarged subependymal veins (Fig. 2C). Postcontrast T1-weighted MR images again showed extensive leptomeningeal enhancement and right choroid plexus



**Figure 1.** Extensive skin manifestation of Sturge–Weber syndrome. Right-sided facial venous malformation (port-wine birthmark) extending to the scalp, ear, and right arm, chest, and back.

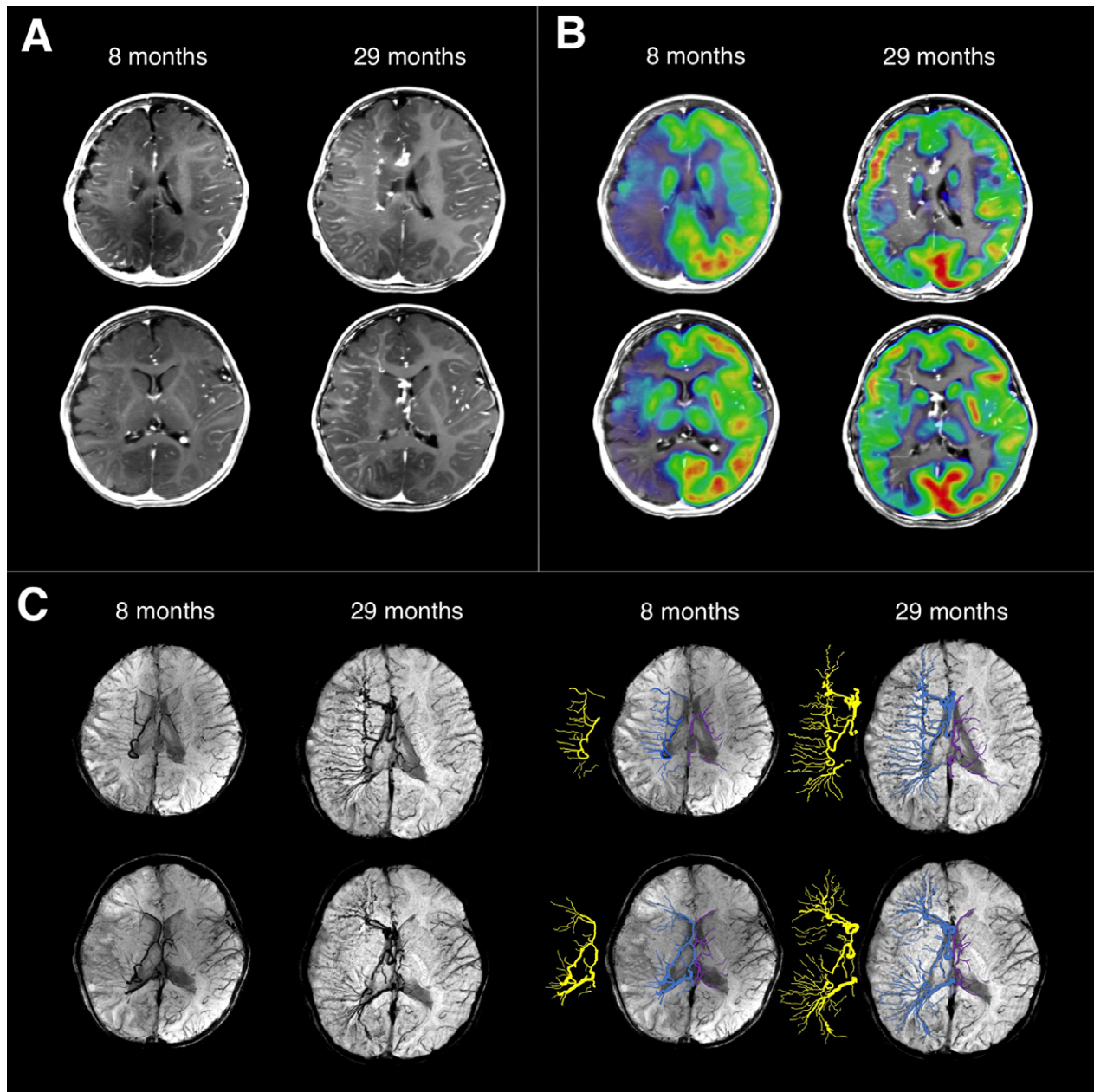


**Figure 2.** Multimodal neuroimaging at age 8 months and 29 months. (A) Postcontrast T1-weighted images showing leptomeningeal enhancement and lack of normal surface veins in the right frontal, parietal, and temporal lobes at both time points. Moreover, the right hemispheric multilobar atrophy at age 29 months seemed to be slightly less pronounced than at age 8 months, with less asymmetric CSF space. (B) On interictal 2-deoxy-2-[<sup>18</sup>F]fluoro-D-glucose (FDG)-PET scans (coregistered with postcontrast T1 images), severe right hemispheric hypometabolism was observed, with a relatively preserved medial frontal and parietal cortex at the age of 8 months. Glucose metabolism at the age of 29 months showed a dramatic improvement of metabolic activity. (C) Susceptibility-weighted imaging (SWI) minimum intensity projection (MIP) images visualized enlarged deep medullary veins in the right hemisphere (enhanced in blue on the right panels, also its skeleton is displayed next to the enhanced images in yellow; contralateral deep medullary veins are enhanced in purple). The right-sided deep veins became much more extensive by 29 months of age, encompassing the whole right hemisphere.

enlargement, and it also visualized numerous medullary veins (Fig. 2A). Perfusion imaging also documented blood flow in the enlarged deep veins. The right hemispheric

multilobar atrophy seemed to be slightly less pronounced than at age 8 months, with less asymmetric CSF space apparent especially in the anterior temporal region

(Fig. 2A). Fiber tractography from diffusion tensor imaging (64 diffusion directions, b-values: 0 and 1000 s/mm<sup>2</sup>, voxel size: 2.0 × 2.0 × 2.0 mm<sup>3</sup>, acquisition time: 9 min 26 s) demonstrated a dominant arcuate fasciculus in the left hemisphere and slightly diminished corticospinal and central visual tracts in the right hemisphere as compared to the left (Fig. 3). FDG-PET scan showed a much-improved metabolic activity throughout the right hemisphere compared to the first scan, with some residual hypometabolism in the parietal and occipital cortex, and slightly higher metabolism in portions of the right frontal and superior temporal cortex as compared to the left (Fig. 2B). EEG recorded during the FDG uptake period showed focal attenuation and slowing of the background activity over the right hemisphere without epileptiform discharges. She remained to have good communication skills (score: 113 on VABS-II), and improved, adequate daily living, socialization, and motor skill scores (104, 100, and 96, respectively). Direct assessment of early learning (using Mullen Scales of Early Learning) estimated her overall cognitive ability in the “very high” range, with relative strengths for expressive language (high average), and receptive language, visual perception, gross and fine motor skills each measured within the average range. She also scored within normal limits across domains on caregiver report of behavioral problems on the Child Behavior Checklist. At the time of paper submission, she was 34 months old, remained seizure-free, and continued to develop well without any new issues on unchanged medication.

## Discussion

Here, we used longitudinal MRI with SWI to demonstrate a robust expansion of deep venous collaterals in the affected right hemisphere of a young child with SWS.

These vascular changes were associated with the recovery of early severe hemispheric glucose hypometabolism along with normalized neurocognitive development following an initial cluster of seizures and motor symptoms. These findings document a massive hemispheric deep venous remodeling during the early SWS disease course and suggest that the expanded deep cerebral venous system may effectively compensate for the blocked superficial hemispheric venous drainage.

Children with SWS are at risk for progressive neurocognitive deficits. Bilateral brain involvement and early-onset, frequent seizures are major predictors of poor clinical outcome.<sup>6,10,11</sup> However, studies in unilateral SWS (representing the majority of SWS cases) suggested effective compensatory mechanisms leading to relatively preserved neurocognitive functioning in a subgroup of patients with extensive damage, presumably due to early functional reorganization in the contralateral (unaffected) hemisphere.<sup>4-6</sup> Contralateral changes have been also documented by FDG-PET in the form of increased cortical metabolism, mostly affecting posterior regions including the visual cortex.<sup>12-14</sup> In addition, DTI fiber tractography studies showed signs of strengthening of the contralateral central motor and visual pathways in some SWS children with preserved motor and visual functions, respectively.<sup>13,15</sup>

In this study, we document the evolution and potential beneficial effects of robust deep cerebral venous expansion evolving after the onset of the first SWS-related seizures. The ability of deep medullary veins to enlarge in the post-natal period of SWS has been demonstrated in our recent study.<sup>8</sup> In those cases, however, the changes were confined to a few enlarged medullary veins located in the frontal lobe. In the present child, the expansion was extensive and robust, involving all four lobes in the affected hemisphere. These vascular changes followed a

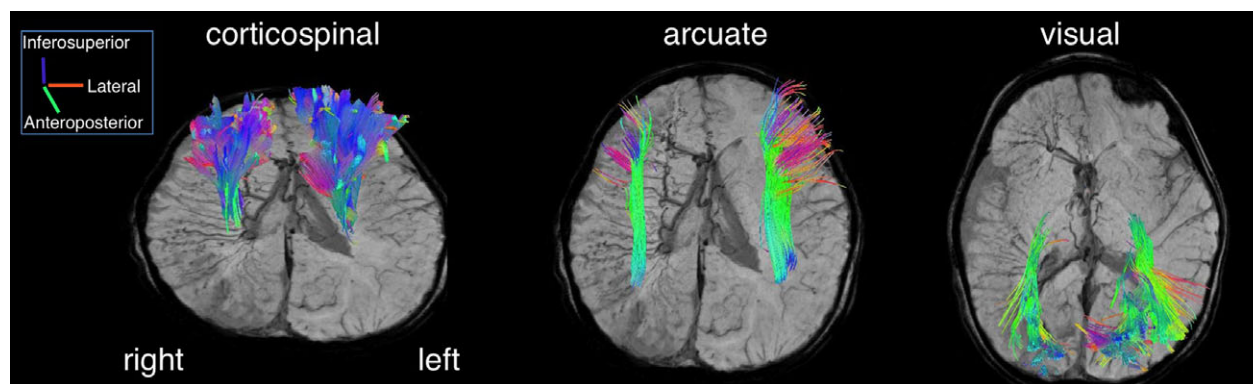


**Figure 3.** Diffusion tensor imaging fiber tractography at 29 months of age (superimposed on SWI images). Three major tracts (corticospinal, arcuate, and central visual), reconstructed in both hemispheres, showed a slight asymmetry with preponderance in the left hemisphere. The direction of the fiber tracts is color-coded.

cluster of initial seizures and prolonged motor weakness associated with severe hemispheric hypometabolism detected by PET weeks after the cessation of seizures. Normalization of hemispheric metabolism was marked (although incomplete) on the follow-up PET scan, and the remaining mild metabolic and structural abnormalities (along with abnormal EEG background activity) were clinically compensated with no apparent neurocognitive or behavioral deficits. It is reasonable to assume that the venous flow compensation provided by the enlarged deep venous system contributed to this remarkable recovery. The mechanisms governing such a massive and effective deep venous remodeling in the early symptomatic disease stage of SWS remain unclear; it is also unknown whether early, aggressive antiepileptic and aspirin treatment contributed to this process. Nevertheless, these data indicate that multilobar expansion of deep cerebral veins in SWS in the symptomatic stage may contribute to reversal of initial neurocognitive deficits in children with extensive unilateral SWS brain involvement.

## Acknowledgment

The authors thank Cynthia Burnett, BA, for assistance with patient scheduling; Jane Cornett, RN, and Anne Deboard, RN, for performing sedation for imaging; Yang Xuan, BS, for MRI acquisition and preprocessing. This work was supported by grants from the National Institutes of Health (R01 NS041922 to C.J. and R01 NS089659 to J.J.).

## Conflict of Interest

The authors declare no competing financial interests.

## References

1. Bodensteiner JB, Roach ES. Overview of Sturge-Weber syndrome. In: Bodensteiner JB, Roach ES, eds. *Sturge-Weber syndrome*. Mt Freedom, NJ: The Sturge-Weber Foundation, 2010:19–32.
2. Shirley MD, Tang H, Gallione CJ, et al. Sturge-Weber syndrome and port-wine stains caused by somatic mutation in GNAQ. *N Engl J Med* 2013;23:1971–1979.
3. Lo W, Marchuk DA, Ball KL, et al. Updates and future horizons on the understanding, diagnosis, and treatment of Sturge-Weber syndrome brain involvement. *Dev Med Child Neurol* 2012;54:214–223.
4. Lee JS, Asano E, Muzik O, et al. Sturge-Weber syndrome: correlation between clinical course and FDG PET findings. *Neurology* 2001;24:189–195.
5. Behen ME, Juhász C, Wolfe-Christensen C, et al. Brain damage and IQ in unilateral Sturge-Weber syndrome: support for a “fresh start” hypothesis. *Epilepsy Behav* 2011;22:352–357.
6. Bosnyák E, Behen ME, Guy WC, et al. Predictors of cognitive functions in children with Sturge-Weber syndrome: a longitudinal study. *Pediatr Neurol* 2016;61:38–45.
7. Tong KA, Ashwal S, Obenaus A, et al. Susceptibility-weighted MR imaging: a review of clinical applications in children. *AJNR Am J Neuroradiol* 2008;29:9–17.
8. Pilli VK, Chugani HT, Juhász C. Enlargement of deep medullary veins during the early clinical course of Sturge-Weber syndrome. *Neurology* 2017;3:103–105.
9. Ye Y, Hu J, Wu D, Haacke EM. Noncontrast-enhanced magnetic resonance angiography and venography imaging with enhanced angiography. *J Magn Reson Imaging* 2013;38:1539–1548.
10. Kramer U, Kahana E, Shorer Z, Ben-Zeev B. Outcome of infants with unilateral Sturge-Weber syndrome and early onset seizures. *Dev Med Child Neurol* 2000;42:756–759.
11. Zabel TA, Reesman J, Wodka EL, et al. Neuropsychological features and risk factors in children with Sturge-Weber syndrome: four case reports. *Clin Neuropsychol* 2010;24:841–859.
12. Batista CE, Juhasz C, Muzik O, et al. Increased visual cortex glucose metabolism contralateral to angioma in children with Sturge-Weber syndrome. *Dev Med Child Neurol* 2007;49:567–573.
13. Jeong JW, Tiwari VN, Shin J, et al. Assessment of brain damage and plasticity in the visual system due to early occipital lesion: comparison of FDG-PET with diffusion MRI tractography. *J Magn Reson Imaging* 2015;41:431–438.
14. Kim JA, Jeong JW, Behen ME, et al. Metabolic correlates of cognitive function in children with unilateral Sturge-Weber syndrome: evidence for regional functional reorganization and crowding. *Hum Brain Mapp* 2017; <https://doi.org/10.1002/hbm.23937>.
15. Kamson DO, Juhász C, Shin J, et al. Patterns of structural reorganization of the corticospinal tract in children with Sturge-Weber syndrome. *Pediatr Neurol* 2014;50:337–342.